

Light-Emitting Cyclopalladated Complexes of 6-Phenyl-2,2'-bipyridines with Hydrogen-Bonding Functionality

Francesco Neve,^{*,†} Alessandra Crispini,[†] Cinzia Di Pietro,[‡] and Sebastiano Campagna^{*,‡}

Dipartimento di Chimica, Università della Calabria, I-87030 Arcavacata di Rende (CS), Italy, and Dipartimento di Chimica Inorganica, Chimica Analitica e Chimica Fisica, Università di Messina, Via Sperone 31, I-98166 Messina, Italy

Received March 13, 2002

The tridentate ligand 4-carboxy-6-phenyl-2,2'-bipyridine (HL1) was used to prepare the cyclometalated Pd(II) complex [Pd(L1)Cl] (**1**). Similar ligands were effective in the formation of [Pd(L2)Cl] (**2**) and [Pd(L3)Cl] (**3**) (where HL2 = 4-carboxyphenyl-6-phenyl-2,2'-bipyridine and HL3 = 4-hydroxyphenyl-6-phenyl-2,2'-bipyridine). The crystal structure of [Pd(L1)Cl]·H₂O has been determined by X-ray diffraction, revealing a variegated array of H-bonding motifs and π -stacking. The [Pd(L1)Cl] molecules are associated in dimers with an intradimer Pd···Pd distance of 3.27 Å, while dimers are separated by interdimer Pd···Pd contacts of 5.41 Å. All complexes **1–3** exhibited intense luminescence at 77 K, with lifetimes in the 10–200 μ s range. The luminescence is assigned to metal-perturbed triplet ligand-centered (LC) excited states for **1** and **3** (partially mixed with an upper-lying metal-to-ligand charge transfer (MLCT) level) and to an excimeric excited state for **2**. Room-temperature solid-state luminescence was also revealed by **1** (emission energy and lifetime of 650 nm and 1 μ s, respectively), which has been assigned to oligomeric species. Differences in the photophysical properties of **1–3** are addressed with reference to the chemical structure and electronic properties of their polypyridine ligands.

Introduction

Luminescent Pd(II) complexes are exceedingly rare if compared to analogous Pt(II) luminophores.¹ With few notable exceptions,^{2,3} most systems emit only at low temperature and with low efficiency.^{4–7} It has also been recognized that when incorporated in polynuclear complexes, Pd(II) centers may lead to partial quenching of luminescence.^{7b,c} Despite these unfavorable premises, several photoactive Pd(II) complexes have been recently the subject of accurate photophysical studies.^{8–10} In particular, cyclometalated species⁹ were designed for

application in organic light-emitting devices (OLED), thus participating in the revived interest for cyclopalladated complexes as potential candidates for optical and electroluminescent devices.^{11–15}

We have recently started an investigation on the luminescence properties of cyclopalladated species which also have mesogenic behavior.^{16–18} All the species under study were of [Pd(L)X] type, where HL are substituted 6-phenyl-2,2'-bipyridine ligands. In this respect, our studies were somewhat complementary to those of Che and co-workers on mononuclear and dinuclear Pt(II) complexes¹⁹ (and only very recently on Pd(II) ana-

* To whom correspondence should be addressed. E-mail: f.neve@unical.it or photochem@chem.unime.it.

[†] Università della Calabria.

[‡] Università di Messina.

(1) (a) Maestri, M.; Balzani, V.; Deuschel-Cornioley, C.; von Zelewsky, A. *Adv. Photochem.* **1992**, *17*, 1. (b) Paw, W.; Cummings, S. D.; Mansour, M. A.; Connick, W. B.; Geiger, D. K.; Eisenberg, R. *Coord. Chem. Rev.* **1998**, *171*, 125.

(2) Wakatsuki, Y.; Yamazaki, H.; Grutsch, P. A.; Santhaman, M.; Kutal, C. *J. Am. Chem. Soc.* **1985**, *107*, 8153.

(3) Ghedini, M.; Pucci, D.; Calogero, G.; Barigelletti, F. *Chem. Phys. Lett.* **1997**, *267*, 341.

(4) (a) Deuschel-Cornioley, C.; Ward, T.; von Zelewsky, A. *Helv. Chim. Acta* **1988**, *71*, 130. (b) Maestri, M.; Sandrini, D.; Balzani, V.; von Zelewsky, A.; Deuschel-Cornioley, C.; Jolliet, P. *Helv. Chim. Acta* **1988**, *71*, 1053. (c) Barigelletti, F.; Sandrini, D.; Maestri, M.; Balzani, V.; von Zelewsky, A.; Chassot, L.; Jolliet, P.; Maeder, U. *Inorg. Chem.* **1988**, *27*, 3644.

(5) Craig, C. A.; Watts, R. J. *Inorg. Chem.* **1989**, *28*, 309.

(6) Guglielmo, G.; Ricevuto, V.; Giannetto, A.; Campagna, S. *Gazz. Chim. It.* **1989**, *119*, 457.

(7) (a) Yam, V. W.-W.; Lee, V. W.-M.; Cheung, K.-K. *Organometallics* **1997**, *16*, 2833. (b) Zahavy, E.; Fox, M. A. *Chem. Eur. J.* **1998**, *4*, 1647. (c) Slone, R. V.; Benkstein, K. D.; Belanger, S.; Hupp, J. T.; Guzei, I. A.; Rheingold, A. L. *Coord. Chem. Rev.* **1998**, *171*, 221.

(8) Lai, S.-W.; Cheung, T.-C.; Chan, M. C. W.; Cheung, K.-K.; Peng, S.-M.; Che, C.-M. *Inorg. Chem.* **2000**, *39*, 255.

(9) (a) Wu, Q.; Hook, A.; Wang, S. *Angew. Chem., Int. Ed.* **2000**, *39*, 3933. (b) Song, D.; Wu, Q.; Hook, A.; Kozin, I.; Wang, S. *Organometallics* **2001**, *20*, 4683.

(10) (a) Yam, V. W.-W.; Zhang, L.; Tao, C.-H.; Wong, K. M.-C.; Cheung, K.-K. *J. Chem. Soc., Dalton Trans.* **2001**, 1111. (b) Yam, V. W.-W.; Tao, C.-H.; Zhang, L.; Wong, K. M.-C.; Cheung, K.-K. *Organometallics* **2001**, *20*, 453.

(11) Ghedini, M.; Pucci, D.; Scaramuzza, N.; Komitov, L.; Lagerwall, S. T. *Adv. Mater.* **1995**, *7*, 659.

(12) Neumann, B.; Hegmann, T.; Tschierske, C. *Chem. Commun.* **1998**, 105.

(13) El-ghayoury, A.; Douce, L.; Skoulios, A.; Ziessel, R. *Angew. Chem., Int. Ed.* **1998**, *37*, 1255.

(14) Omnes, L.; Timini, B. A.; Gelbrich, T.; Hursthouse, M. B.; Luckhurst, G. R.; Bruce, D. W. *Chem. Commun.* **2001**, 2248.

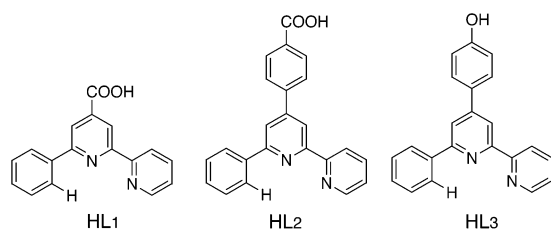
(15) Aiello, I.; Dattilo, D.; Ghedini, M.; Golemme, A. *J. Am. Chem. Soc.* **2001**, *123*, 5598.

(16) Neve, F.; Ghedini, M.; Crispini, A. *Chem. Commun.* **1996**, 2463.

(17) Neve, F.; Crispini, A.; Campagna, S. *Inorg. Chem.* **1997**, *36*, 6150.

(18) Neve, F.; Ghedini, M.; Francescangeli, O.; Campagna, S. *Liq. Cryst.* **1998**, *24*, 673.

Chart 1



logues⁸) containing similar ligands. While luminescence in a glass matrix at 77 K was always observed, we found that our cyclopalladated species were emissive also in the solid state at room temperature.^{17,18} Interpretation of the photophysical data however led us to suggest that “isolated molecules” were responsible for the solid-state emission process from these mononuclear compounds. To improve the emissive properties of the organopalladates, we have chosen functionalized 6-phenyl-2,2'-bipyridine ligands (HLn (n = 1–3), Chart 1) that may promote intermolecular contacts through hydrogen bonding and/or π -stacking. The photophysical properties of the resulting cyclometalated [Pd(Ln)Cl] complexes are now presented and discussed, also taking advantage of the solid-state characterization of one of them.

Results and Discussion

The ligands used in this study were prepared through classical Kröhnke-type²⁰ syntheses. The reactions were single-step (HL1) or multistep^{18,21} processes (HL2 and HL3). All the preparations led to the desired product in good overall yield (50–70%), an outcome not always achieved for oligopyridines prepared with this general method.²² The metalated derivatives [Pd(L1)Cl] (**1**), [Pd(L2)Cl] (**2**), and [Pd(L3)Cl] (**3**) were obtained as yellow microcrystalline solids by reaction of [Pd(PhCN)₂Cl₂] and the HL ligands in a methanol/benzene mixture. Due mainly to the different solubility properties of the ligands, while the formation of both **1** and **2** required reflux conditions, **3** was obtained at room temperature. The use of [Pd(PhCN)₂Cl₂] as a precursor for cyclopalladated products containing a chloride ligand has proved somewhat superior with respect to other reagents such as [PdCl₄]²⁻ alkali salts or Pd(OAc)₂, as shorter reaction times and milder conditions are usually required. Apart from DMSO, common organic solvents are not good solvents for compounds **1–3**. Compound **1** is also slightly soluble in CH₂Cl₂ and acetone.

Single crystals of compounds **1–3** are very difficult to grow. We succeeded for **1** but only after several painstaking attempts. Yellow-orange crystals of **1** were grown by very slow evaporation from a diluted acetone solution. **1** crystallized as a monohydrate, and the role of water in the crystal packing of **1** will become more clear in the next section. The water uptake seems to be a spontaneous process and, more importantly, characteristic of both the yellow-orange crystals grown from acetone and the yellow microcrystalline solid formed from the reaction mixture. In both cases, cocrystallized water may come from residual water in the solvent. Although indirectly, inclusion of water in the microcrystalline solid was tested by infrared spectroscopy. In addition to a very broad band in the region of O–H stretching (3600–2500 cm⁻¹), the IR spectrum (KBr pellet) exhibited a strong absorption band at 1707 cm⁻¹ (with a shoulder at ~1730 cm⁻¹) that can be assigned to the C=O stretching of the carboxylic acid group of the coordinated L1 ligand. Upon heating the KBr pellet at 160 °C in a vacuum for 2 h and collecting the spectrum immediately after, the IR spectrum revealed a new strong ν (C=O) absorption band (with two close maxima at 1752 and 1738 cm⁻¹) in addition to the original one at 1705 cm⁻¹. Interestingly, the initial IR spectrum was restored barely leaving the pellet in air for 1 h. The substantial variation of the ν (C=O) value upon heating **1** is a likely hint for the presence of water molecules strongly associated with the carboxylic acid group in the molecule, a fact that is also indirectly confirmed by the resistance to complete water loss under the experimental conditions.²³ Thus, the microcrystalline **1** may contain water, which is partially lost on heating and which is readsorbed from the air when the sample is cooled back to room temperature. Similar changes in the infrared spectrum were also noted for the crystalline yellow-orange form of **1**. In both cases, no color changes were observed during the solvent release–uptake cycle. Finally, it must be noted that a thermal treatment similar to that of **1** gave no notable changes in the IR spectrum of complex **2**, leaving the strong ν (C=O) absorption band (featuring two maxima at 1684 and 1697 cm⁻¹) unaffected.

Crystal Structure of 1. The structure of **1** has been determined by X-ray crystallography. The molecule is nearly flat (except for the carboxy group) with the palladium atom in a distorted square-planar coordination geometry (Figure 1). Metal–ligand distances are similar to those observed for other Pd(II) complexes of cyclometalating 6-phenyl-2,2'-bipyridine ligands.^{8,16,24} The bite angle value of the chelating L1 ligand (N(1)–Pd–C(12), 160.0°) is also typical for the above systems and compares well to that of related N \wedge N \wedge N,²⁵ N \wedge N \wedge C,²⁶

(19) (a) Cheung, T.-C.; Cheung, K.-K.; Peng, S.-M.; Che, C.-M. *J. Chem. Soc., Dalton Trans.* **1996**, 1645. (b) Liu, H.-Q.; Cheung, T.-C.; Che, C.-M. *Chem. Commun.* **1996**, 1039. (c) Wu, L.-Z.; Cheung, T.-C.; Che, C.-M.; Cheung, K.-K.; Lam, M. H. W. *Chem. Commun.* **1998**, 1127. (d) Tse, M.-C.; Cheung, K.-K.; Chan, M. C. W.; Cheung, K.-K.; Che, C.-M. *Chem. Commun.* **1998**, 2295. (e) Lai, S.-W.; Chan, M. C.-W.; Cheung, T.-C.; Che, C.-M. *Organometallics* **1999**, *18*, 3327. (f) Lai, S.-W.; Chan, M. C.-W.; Cheung, T.-C.; Peng, S.-M.; Che, C.-M. *Inorg. Chem.* **1999**, *38*, 4046. (g) Wong, K. H.; Chan, M. C. W.; Che, C.-M. *Chem. Eur. J.* **1999**, *5*, 2845. (h) Lu, W.; Chan, M. C. W.; Cheung, K.-K.; Che, C.-M. *Organometallics* **2001**, *20*, 2477. (i) Lai, S.-W.; Lam, H.-W.; Lu, W.; Cheung, K.-K.; Che, C.-M. *Organometallics* **2002**, *21*, 226. (j) Lu, W.; Mi, B.-X.; Chan, M. C. W.; Hui, Z.; Zhu, N.; Lee, S.-T.; Che, C.-M. *Chem. Commun.* **2002**, 206.

(20) Kröhnke, F. *Synthesis* **1976**, 1.

(21) Neve, F.; Crispini, A.; Campagna, S.; Serroni, S. *Inorg. Chem.* **1999**, *38*, 2250.

(22) Alternative procedures based on a highly competitive solventless approach have been recently reviewed: Cave, G. W. V.; Raston, C. L.; Scott, J. L. *Chem. Commun.* **2001**, 2159.

(23) More severe conditions (heating at 180 °C for 72 h) resulted in a slightly different behavior, since complete recovery of the initial spectrum was only obtained after waiting a much longer time. Indeed, the presence of carboxyl acid dimers in the solid state (that would account for equally strongly H-bonded acid groups and therefore IR stretching bands of similar magnitude) cannot be completely discarded. In the latter case, a prediction of the actual role of water in the crystal packing is very difficult.

(24) Constable, E. C.; Henney, R. P. G.; Leese, T. A.; Tocher, D. A. *J. Chem. Soc., Chem. Commun.* **1990**, 513.

(25) (a) Ramdeehul, S.; Barloy, L.; Osborn, J. A.; De Cian, A.; Fischer, J. *Organometallics* **1996**, *15*, 5442. (b) Barloy, L.; Gauvin, R. M.; Osborn, J. A.; Sizun, C.; Graff, R.; Kyritsakas, N. *Eur. J. Inorg. Chem.* **2001**, 1699.

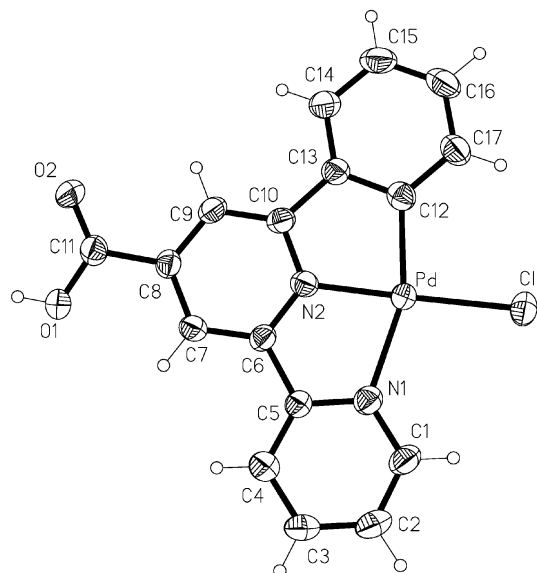
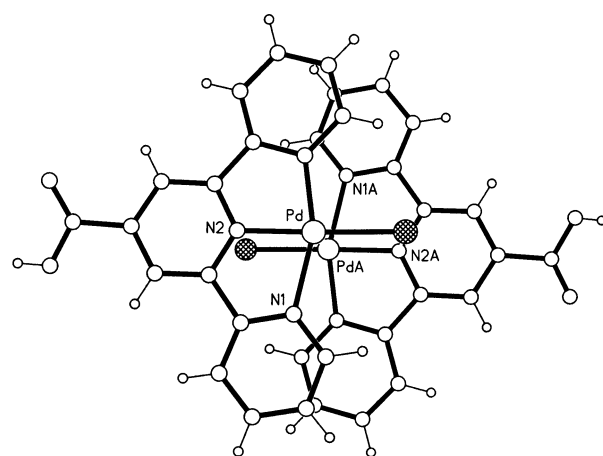


Figure 1. Perspective view of **1** with thermal ellipsoids drawn at the 50% probability level. Selected bond lengths (Å) and angles (deg): Pd–N(1), 2.150(3); Pd–N(2), 1.964(3); Pd–C(12), 1.997(4); Pd–Cl, 2.334(1); C(11)–O(1), 1.311(4); C(11)–O(2), 1.210(5); N(1)–Pd–N(2), 78.6(1); N(2)–Pd–C(12), 81.4(1); N(1)–Pd–C(12), 160.0(1); N(2)–Pd–Cl, 177.5(1); O(1)–C(11)–O(2), 124.3(3).

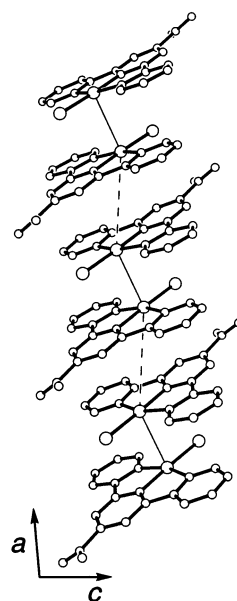
$\text{N}\wedge\text{C}\wedge\text{N}$,²⁷ or $\text{C}\wedge\text{N}\wedge\text{C}$ ²⁸ tridentate ligands with similar geometric constraints.

The crystal structure of **1** consists of inversion-related dimers with a Pd···Pd intradimer contact of 3.27 Å (Figure 2a), a value slightly larger than the sum of their van der Waals radii.²⁹ The molecules within the dimer are arranged in a head-to-tail fashion. The Pd–Pd vector is essentially orthogonal to the coordination plane (1° angle with the plane normal), suggesting a weakly attractive character for the M···M interaction. The latter also shows a small degree of pyramidalization ($\alpha = 91.0^\circ$) according to Aullon et al.^{30a} In fact, intermolecular d^8 – d^8 short contacts are less common for mononuclear square-planar palladium complexes,^{30b} which testifies to the lower ability of Pd(II) species to electronically interact in the solid state with respect to the corresponding Pt(II) analogues.³¹

Intermolecular contact also occurs through aromatic π – π stacking within the dimer. The stacking interaction (best seen in Figure 2a) involves both the external pyridine and the metalated phenyl ring of the L1 ligand in each molecule, giving rise to offset arene–pyridine dimeric π -stacks. The slipped geometry of the aromatic interaction (interplanar distance 3.34 Å) is characterized by a centroid–centroid distance of 3.73 Å, interplanar



(a)



(b)

Figure 2. (a) Diagram showing the slipped face-to-face π – π interaction in the dimeric unit of **1**. (b) Stacking arrangement of Pd₂ dimers along the *a* axis with alternation of short (solid lines) and long (dashed lines) Pd–Pd contacts.

angle of 2.8°, displacement angle of 27°, and horizontal slip of 1.66 Å. Ring slippage leads to C–C or C–N contacts of 3.41–3.62 Å, that is, within the range expected for fairly strong aromatic interactions with parallel displaced arrangement of the rings.³² Although less effective, aromatic stacking extends beyond the dimeric units. The Pd₂ dimers stack along the *a* axis (Figure 2b), bringing the interplanar distance between two consecutive dimers to 3.45 Å. The interdimer stacking is of pyridine–pyridine type,^{32b} and it occurs through the central pyridine ring of the L1 ligand. The weaker interaction is slipped, parallel displaced (centroid–centroid distance, 4.63 Å, displacement angle of

(26) (a) Butler, I. R. *Organometallics* **1992**, *11*, 74. (b) Isaac, C. J.; Price, C.; Horrocks, B. R.; Houlton, A.; Elsegood, M. R. J.; Clegg, W. *J. Organomet. Chem.* **2000**, *598*, 248.

(27) Cardenas, D. J.; Echavarren, A. M.; Ramirez de Arellano, M. C. *Organometallics* **1999**, *18*, 3337.

(28) (a) Newman, C. P.; Cave, G. W. V.; Wong, M.; Errington, W.; Alcock, N. W.; Rourke, J. P. *J. Chem. Soc., Dalton Trans.* **2001**, 2678. (b) Lu, W.; Chan, M. C. W.; Cheung, K.-K.; Che, C.-M. *Organometallics* **2001**, *20*, 2477. (c) Peris, E.; Loch, J. A.; Mata, J.; Crabtree, R. H. *Chem. Commun.* **2001**, 201.

(29) Bondi, A. J. *J. Chem. Phys.* **1964**, *68*, 441.

(30) (a) Aullon, G.; Alemany, P.; Alvarez, S. *Inorg. Chem.* **1996**, *35*, 5061. (b) Aullon, G.; Alvarez, S. *Chem. Eur. J.* **1997**, *3*, 655.

(31) Houlding, V. H.; Miskowski, V. M. *Coord. Chem. Rev.* **1991**, *111*, 145.

(32) (a) Hunter, C. A.; Sanders, J. K. M. *J. Am. Chem. Soc.* **1990**, *112*, 5525. (b) Janiak, C. J. *J. Chem. Soc., Dalton Trans.* **2000**, 3885. (c) Hunter, C. A.; Lawson, K. R.; Perkins, J.; Urch, C. J. *J. Chem. Soc., Perkin Trans. 2* **2001**, 651. (d) Tsuzuki, S.; Honda, K.; Uchimar, T.; Mikami, M.; Tanabe, K. *J. Am. Chem. Soc.* **2002**, *124*, 104.

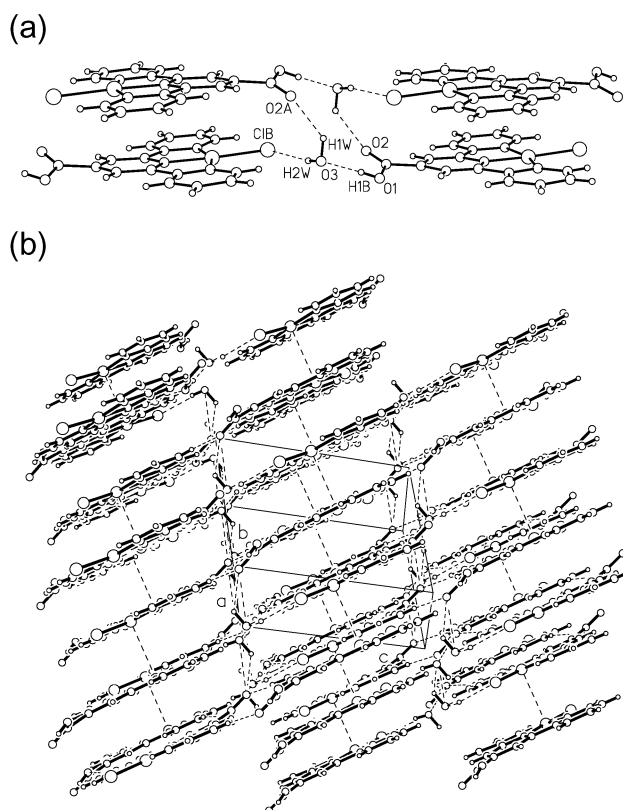
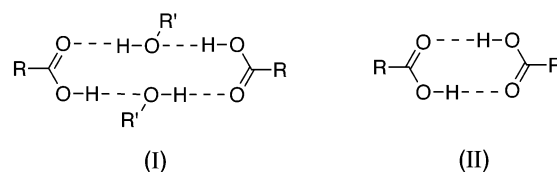


Figure 3. (a) H-bonding pattern revealed by $1 \cdot \text{H}_2\text{O}$. Hydrogen bond lengths (Å) and angles (deg) (with symmetry codes): O1–H1B \cdots O3 [H \cdots O 1.76, O \cdots O 2.581(4), O–H \cdots O 176], O3–H1W \cdots O2A(3+x, 1–y, 2+z) [H \cdots O 2.15(4), O \cdots O 2.918(4), O–H \cdots O 138], O3–H2W \cdots C1B(1+x, y, 1+z) [H \cdots Cl 2.26(3), O \cdots Cl 3.176(4), O–H \cdots Cl 161]. (b) View emphasizing the lamellar arrangement of the crystal packing. Dashed lines represent the short Pd–Pd contacts.

42° , and horizontal slip of 3.1 Å), leading to shortest contacts in the range 3.52–4.00 Å. The corresponding interdimer Pd \cdots Pd distance is 5.41 Å. Intra- and interdimer Pd–Pd contacts thus alternate along a zigzag chain (Pd–Pd(a)–Pd, 131°). In this regard, the packing behavior of **1** resembles that of [Pt(L)(MeCN)]PF₆ (HL = 6-phenyl-2,2'-bipyridine) (intradimer and interdimer distances of 3.28 and 4.59 Å, respectively)²⁴ and [Pt-(terpy)Cl]ClO₄ (terpy = 2,2':6',2''-terpyridine) (intradimer and interdimer distances of 3.27 and 4.20 Å, respectively)³³ more than that of [Pd(L)Cl]⁵ and [Pd(L4)Cl] (HL4 = 4-(4'-dodecyloxyphenyl)-6-phenyl-2,2'-bipyridine),¹⁶ which revealed no short Pd–Pd contacts. Taking into account both the metal–metal and the aromatic π – π stacking, the crystal packing of **1** can be described in terms of discrete M–M units within an infinite π -stacking. Going back to the role of cocrystallized water, this brings into evidence the importance of hydrogen bonding in the supramolecular organization of **1**. Since the cyclometalated L1 ligand bears a single carboxylic acid group, the latter is expected to participate in intermolecular hydrogen bonding with a carboxylic acid group from a neighboring molecule. Pairing indeed occurs although mediated by water molecules (Figure 3a), affording an R₄⁴(12) cyclic motif^{34–36} (I in Chart 2) instead of the more familiar R₂²(8) ring³⁷ (II

(33) Bailey, J. A.; Hill, M. G.; Marsh, R. E.; Miskowski, V. M.; Schaefer, W. P.; Gray, H. B. *Inorg. Chem.* **1995**, *34*, 4591.

Chart 2



in Chart 2). Within the centrosymmetric R₄⁴(12) ring, short^{38,39} O–H \cdots O bonds (H \cdots O, 1.76 Å; O \cdots O, 2.58 Å) alternate with longer ones (H \cdots O, 2.15 Å; O \cdots O, 2.92 Å). Intermolecular C–H \cdots O interactions (with H \cdots O contacts in the range 2.4–2.6 Å) were also observed that involve the oxygen atoms of both the water molecule and the carboxylic acid group.

Since the inclusion of water increases the number of hydrogen bond donors in the system, a further intermolecular interaction must be considered. The water molecule is also H-bonded to the chloride ligand of an adjacent molecule (Figure 3a) through a relatively short⁴⁰ O–H \cdots Cl–Pd contact (H \cdots Cl, 2.26 Å). This interaction leads to the formation of infinite organometallic chains (although with interleaving water molecules) running parallel to the [101] direction. This supramolecular motif is reminiscent of the infinite organometallic chains formed through intermolecular H \cdots Cl–Pt hydrogen bonds in Pt(II) pincers functionalized with hydrogen bond donors.⁴¹

Since all different aspects of the crystal structure of **1** have been considered individually, it is perhaps also useful to draw an overall picture. Molecules self-assemble in the solid state using all types of assembling functions available (i.e., hydrogen bond donors and acceptors, aromatic π -stacking, coordinatively unsaturated metal centers) including solvent inclusion. Thus all interactions cooperate in the stabilization of stacking. As a result, a lamellar-type structure is formed (Figure 3b), with in-plane intermolecular H-bonding and with tight intermolecular contacts (between metals, between aromatics, and again H-bonding) holding the lamellae together. As will be discussed later, intermolecular interactions seem to show a relevant effect on the solid-state luminescence properties of complex **1**.

(34) For a description of hydrogen-bond patterns in terms of graph-set theory, see: Etter, M. C.; MacDonald, J. C.; Bernstein, J. *Acta Crystallogr.* **1990**, *B46*, 256.

(35) (a) Weber, E.; Csöregi, I.; Stensland, B.; Czugler, M. *J. Am. Chem. Soc.* **1984**, *106*, 3297. (b) Sueur, S.; Lagrenee, M.; Abraham, F.; Bremard, C. *J. Heterocycl. Chem.* **1987**, *24*, 1285. (c) Baggio, R.; Garland, M. T.; Pereg, M. *Inorg. Chem.* **1997**, *36*, 950. (d) Sugahara, M.; Sada, K.; Miyata, M. *Chem. Commun.* **1999**, 293.

(36) Rare examples of the graph set R₄⁴(12) in inorganic and organic–inorganic compounds have been recently reported. See, respectively: (a) Qin, Z. Q.; Jennings, M. C.; Puddephatt, R. J.; Muir, K. W. *Cryst. Eng. Comm. (web edition)* **2000**, article 11. (b) Angeloni, A.; Orpen, A. G. *Chem. Commun.* **2001**, 343.

(37) (a) Leiserowitz, L. *Acta Crystallogr.* **1976**, *B32*, 775. (b) Braga, D.; Grepioni, F.; Sabatino, P.; Desiraju, G. *Organometallics* **1994**, *13*, 3532. (c) Schneider, W.; Bauer, A.; Schmidbaur, H. *Organometallics* **1996**, *15*, 5445. (d) Tse, M.-C.; Cheung, K.-K.; Chan, M. C. W.; Cheung, K.-K.; Che, C.-M. *Chem. Commun.* **1998**, 2295.

(38) Jeffrey, G. A. *An Introduction to Hydrogen Bonding*; Oxford University Press: New York, 1997.

(39) Vishweshar, P.; Nangia, A.; Lynch, V. M. *Chem. Commun.* **2001**, 179.

(40) (a) Steiner, T. *Acta Crystallogr.* **1998**, *B54*, 456. (b) Brammer, L.; Bruton, E. A.; Sherwood, P. *Cryst. Growth Des.* **2001**, *1*, 277.

(41) (a) James, S. L.; Verspui, G.; Spek, A. L.; van Koten, G. *Chem. Commun.* **1996**, 1309. (b) Davies, P. J.; Veldman, N.; Grove, D. M.; Spek, A. L.; van Koten, G. *Angew. Chem., Int. Ed. Engl.* **1996**, *35*, 1959.

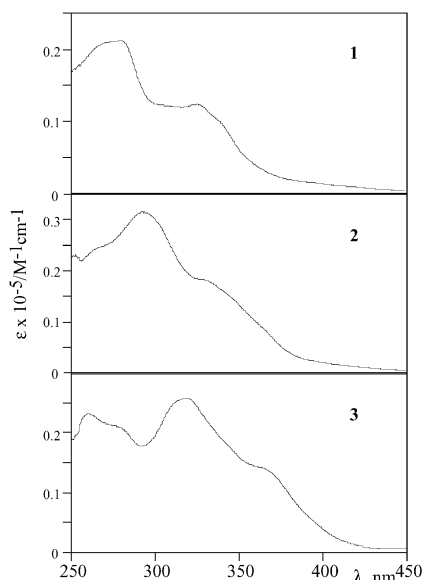


Figure 4. Absorption spectra in DMSO solution of **1** (top), **2** (middle), and **3** (bottom).

Table 1. Spectroscopic and Photophysical Data for Complexes 1–3

compound	absorption ^a		luminescence		
	λ_{\max} , nm	$(\epsilon, \text{M}^{-1} \text{cm}^{-1})$	λ_{\max} , nm	$(\tau, \mu\text{s})$	
1 , [Pd(L1)Cl]	278	(21 100)	510	(40)	glass matrix, ^b 77 K
	326	(12 100)	650	(1)	
2 , [Pd(L2)Cl]	295	(31 200)	610	(15)	glass matrix, ^b 77 K
	332	(17 600)			
3 , [Pd(L3)Cl]	280	(20 700)	495	(170)	glass matrix, ^b 77 K
	320	(25 700)			
	368	(13 600)			

^a In DMSO. ^b DMF/toluene (1:1 v/v).

Absorption Spectra and Luminescence Properties. The absorption spectra of complexes **1–3** in DMSO solution (Figure 4, Table 1) are dominated by intense bands in the visible region (ϵ in the range 10^4 – $10^5 \text{ M}^{-1} \text{ cm}^{-1}$), which can be attributed to spin-allowed metal-perturbed ligand-centered (LC) transitions by comparison with the spectra of Pd(II) complexes with similar polypyridine ligands.^{16–18} At longer wavelengths, less intense shoulders are present, which can receive contribution from spin-allowed metal-to-ligand charge-transfer (MLCT) transitions. The absorption spectra of the compounds in dichloromethane are qualitatively similar to those in DMSO, although the poor solubility in the chlorinated solvent inhibited a more detailed analysis of the spectra, including the calculation of the molar absorption coefficients. None of the new complexes **1–3** exhibit appreciable luminescence in fluid solution at room temperature in any of the solvents employed (dichloromethane, DMF, DMSO).⁴² On the contrary, all of them exhibit strong luminescence in a DMF/toluene (1:1, v/v) rigid matrix at 77 K, with monoexponential lifetimes in the 10^{-5} – 10^{-3} s time range (see Table 1). Interestingly, the emission spectrum of **2** is unstructured, red-shifted, and shorter-lived compared to those of **1** and **3** (Figure 5). Microcrystalline

(42) Actually, a very weak emission around 500 nm was detected for all the species in DMSO and dichloromethane. However, the emission output was at the limit of the sensitivity of our equipment and therefore was not considered.

Table 2. Crystallographic Data for Complex 1

1·H₂O	
empirical formula	C ₁₇ H ₁₃ ClN ₂ O ₃ Pd
fw	453.14
cryst syst	triclinic
space group	<i>P</i> $\bar{1}$
<i>a</i> , Å	7.9364(16)
<i>b</i> , Å	9.4593(19)
<i>c</i> , Å	11.247(2)
α , deg	111.05(3)
β , deg	94.59(3)
γ , deg	98.40(3)
<i>V</i> , Å ³	771.5(3)
<i>Z</i>	2
<i>D</i> (calcd), g/cm ³	1.873
μ , mm ⁻¹	1.394
temp, K	298
wavelength, Å	0.71073
<i>F</i> (000)	432
scan type	θ – 2θ
transm factors	0.45–0.61
no. measd reflns	2634
no. unique reflns	2435 [<i>R</i> (int) = 0.0288]
no. of reflns with $I > 2\sigma(I)$	2328
no. of refined params	223
<i>R</i> indices ^{a,b}	<i>R</i> 1 = 0.0286, w <i>R</i> 2 = 0.0762
<i>R</i> indices (all data)	<i>R</i> 1 = 0.0299, w <i>R</i> 2 = 0.0771
goodness-of-fit	1.11

^a $R1 = \sum(|F_o| - |F_c|) / \sum |F_o|$. ^b $wR2 = [\sum w(F_o^2 - F_c^2)^2 / \sum w(F_o^2)^2]^{1/2}$.

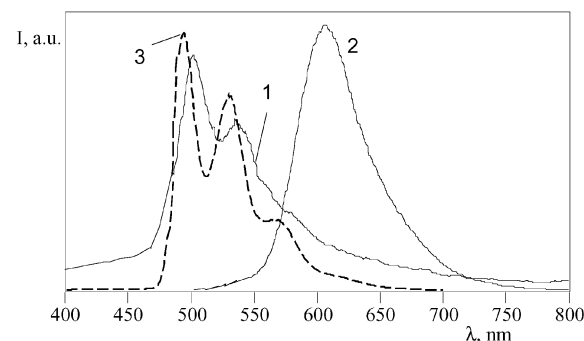


Figure 5. Luminescence spectra of **1–3** in a DMF/toluene (1:1 v/v) rigid matrix at 77 K.

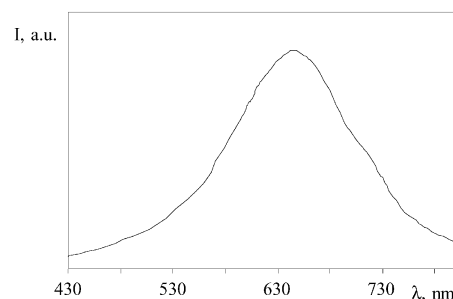


Figure 6. Luminescence spectrum of **1** in the solid state at room temperature.

samples of **1** also exhibit an unstructured room-temperature emission spectrum peaking at 650 nm (Figure 6), significantly red-shifted relative to the emission in a rigid matrix at low temperature. In all the media, the luminescence spectra are independent of the excitation wavelength.

Room-temperature luminescence of mononuclear Pd(II) complexes is very rare,^{2,3} usually because of the presence of low-lying metal-centered (MC) excited states which deactivate the potentially luminescent metal-to-ligand charge transfer (MLCT) and ligand-centered (LC)

levels through thermally activated surface-crossing processes. In fact, MC states have very distorted geometries compared to those of the ground state, so that the Franck–Condon factors for radiationless decay are extremely high and make the radiative processes uncompetitive.⁴³ This problem (common to several transition metal complexes) has proved to be very important for Pd(II) species, so that the cyclometalated approach alone, although useful for several Pt(II) species,^{4,9,17,19} has not been sufficient to favor room-temperature luminescence for Pd(II) compounds.^{5,8,9,16–18} The lack of luminescence for **1–3** at room temperature in fluid solution is therefore not surprising.

The luminescence data of a microcrystalline sample of **1** (in particular the emission energy; see Table 1 and Figure 6) directly suggest that the emission from this species in the solid state can be attributed to excimeric species. Excimer formation (particularly in the solid state) for square-planar metal complexes has been reported to be quite effective in generating room-temperature luminescence.^{19,33,44} Excimeric excited states are indeed substantially red-shifted from MLCT or LC states related to “isolated” molecules, so that the energy gap between the excimeric state and the deactivating MC states increases (as a result, the thermally activated processes involving nonemissive MC levels are inhibited). The reported excimeric emission from square-planar complexes is of two types: (i) charge transfer emission arising from excited states exhibiting substantial metal–metal interaction (metal–metal to ligand charge transfer, MMLCT, sometimes designed as $d\sigma^* \rightarrow \pi^*(\text{ligand})$ charge transfer excited states, where the donor orbital is derived from direct metal–metal interaction) and (ii) $\pi\pi^*$ emission from excited states derived from stacking interactions between the aromatic moieties of the coordinated ligands.^{45,46} In some cases, oligomerization can also occur in the ground state, and in these cases the term “excimer” should be considered in a broader sense.⁴⁵ Since the emission spectra are usually unstructured, and also the emission energies are expected to be similar, a clear distinction between these two types of contribution to the emission is not a trivial task from an experimental viewpoint. X-ray single-crystal data, which indicate both the formation of dimers with short intradimer Pd··Pd contacts and extended π -stacking, would suggest that in principle

either excimeric contribution to the emission is possible. Yet, it should be considered that the luminescence experiments were carried out on the yellow microcrystalline form of **1**; thus we cannot exclude that the arrangement of the molecules in the microcrystalline sample is somewhat different from that obtained from the crystallographic study. Hence, X-ray data alone cannot support a definitive attribution. Furthermore, this is the first time that an excimeric emission at room temperature is reported for Pd(II) complexes, ruling out the possibility of any direct comparison. In conclusion, we cannot safely assign the luminescence of **1** in the solid state either to a specific state (MMLCT or $\pi\pi^*$) or to a mixture of both.

Unlike **1**, compounds **2** and **3** do not exhibit room-temperature emission in the solid state, probably because of a significantly different crystal packing. Major differences in the solid-state supramolecular organization must be expected as a result of several factors. These include a different number of aromatic rings in the cyclometalated ligand (L1 vs L2 and L3), the uneven efficiency of H-bonding groups (L1 and L2 vs L3), and the inclusion of solvent in the crystal lattice. A further reason may be electronic in nature. In this regard, it is useful to recall that the polypyridine ligand L1 has orbitals (both π and π^*) lower in energy than those of L2 and L3, and it is also a much more electron-withdrawing ligand than both L2 and L3, as suggested by the photophysical data reported for cyclometalated Ir(III) complexes based on similar ligands.⁴⁶ These two factors may have consequences relevant to dimer or excimer formation: aromatic interactions can be affected by the energies of the interacting orbitals, and the different electron density on the palladium centers (lower for **1** compared to **2** and **3**) can influence metal–metal interactions.

The picture is quite different at 77 K in rigid matrix, where the thermally activated process involving the MC states cannot occur. Luminescence of **1** and **3** can be safely attributed to metal-perturbed ³LC states on the basis of the structured spectra, energies, and lifetimes (Table 1, Figure 5).^{4–6,8} However, the lifetime of **1** is probably too short to be attributed to a pure (although metal-perturbed) LC state. Most likely the emitting level is mixed with a close-lying, upper MLCT, which influences the excited-state dynamics by decreasing the luminescence lifetime.⁴⁷ A similar mixing is less effective for **3**, because the MLCT state is expected to lie at higher energy than the analogous level in **1**.

The 77 K emission of **2** (Table 1, Figure 5) is very different from those of **1** and **3**. Because of the emission energy, spectrum, and lifetime, it is attributed to $\pi\pi^*$ excimeric states. Such an attribution is also based on the agreement with the photophysical properties recently reported for a series of dimeric Pd(II) complexes,⁸ where excimer formation is favored by structural conformation and excimeric emission is observed at 77 K. Interestingly, no emission features at higher energy are present in the emission spectrum of **2** even changing the concentration, thus suggesting that the equilibrium between “isolated” single molecules and the excimers

(43) Crosby, G. R. *Acc. Chem. Res.* **1975**, *8*, 231.

(44) Kunkely, H.; Vogler, A. *J. Am. Chem. Soc.* **1990**, *112*, 5625.

(45) In principle, an excimer is formed by the combination of a ground-state molecule with an excited-state molecule, a process quite common for aromatic systems (for example, see: Klessinger, M.; Michl, J. *Excited States and Photochemistry of Organic Molecules*; VCH: New York, 1995). The excimer luminescence is expected to be at longer wavelengths than the monomer luminescence, and the associated emission band is commonly broad and without vibrational structure owing to a transition into the unbound ground state. As an excited-state process, excimer formation also competes with other deactivating processes of the initially formed excited state of the monomer. It should be noted that while this definition fully fits the $\pi\pi^*$ luminescence derived from interactions between aromatic moieties (one of them being in its own excited state), the term “excimeric emission” is not formally correct for a MMLCT excited state, for which a metal–metal interaction in the ground state is usually considered. The latter would be more appropriately described as the excited state of a dimeric (or oligomeric) discrete system. However, since in the literature MMLCT emission is very often also called excimeric emission, we decided to use this term in this larger meaning also here, although formal differences should not be forgotten.

(46) Neve, F.; Crispini, A.; Loiseau, F.; Campagna, S. *J. Chem. Soc., Dalton Trans.* **2000**, 1399.

(47) The influence of higher-energy excited states on the dynamics of emitting states by mixing between the states, with minimal perturbation on the emission energy, is well known. For example, see ref 6.

strongly favors excimer formation under these conditions, at least within the studied range of concentration (10^{-5} – 10^{-4} M). The differences in the low-temperature luminescence properties along this series of complexes warrant some additional comment. Extension of the aromatic framework (although not a rigid one) obviously may be an important factor in the formation of the excimer, so that it is not surprising that complex **1** does not show excimeric emission. In contrast, the absence of excimeric emission for **3** calls for a different reason. This might be related to the nature of the substituent on the phenyl ring not involved in metal coordination. We suggest that for complex **2** a key role could be played by hydrogen bonding between carboxyl groups of different molecules (leading to carboxyl dimers at low temperature), which would assist the intermolecular π – π association responsible for the excimeric emission.

Conclusion

In summary, we have exploited the well-known ability of 6-phenyl-2,2'-bipyridine ligands to afford cyclopalladated products.^{16,24} Such cyclometalating ability, coupled to the presence of hydrogen-bond donor (COOH or OH) and acceptor (M–Cl bond) groups on opposite sides of the molecule, enables the potential formation of several intermolecular contacts. While complete structural characterization was not achieved for all complexes, it is apparent that complex **1** fulfills our best expectations relative to the maximization of metal–metal, ligand–ligand, and H-bonding interactions.

Luminescence of complexes **1–3** at 77 K has variable character with respect to the different ligands, being related to excited states of different nature. Solid-state luminescence at room temperature was revealed by **1**, which has been ascribed to an excimeric emission. Since this is the first time this behavior has been proved for a Pd(II) organometallic complex, we are confident that future improvements may allow the consideration of thermally and chemically stable Pd(II) organometallics for light-emitting devices.

Experimental Section

General Methods. All reactions were carried out under a nitrogen atmosphere. ¹H NMR spectra were recorded at room temperature on a Bruker AC 300 spectrometer with tetramethylsilane as internal standard. FT-IR spectra were recorded on a Perkin-Elmer 2000 spectrophotometer for KBr pellets. Elemental analyses were performed using a Perkin-Elmer 2400 microanalyzer. Absorption spectra were recorded with a Kontron Uvikon 860 spectrophotometer, and luminescence spectra were performed with a Jobin Yvon-Spex Fluoromax 2 fluorimeter equipped with a Hamamatsu R3896 photomultiplier. The spectra were corrected for phototube response by using a standard lamp. For the luminescence lifetimes at room temperature, an Edinburgh OB900 time-correlated single-photon-counting spectrometer was employed (nitrogen discharge, pulse width, 4 ns). Luminescence lifetimes at 77 K (μ s time scale) were measured by a Perkin-Elmer 5B spectrofluorimeter with variable delay times (typically between 10 μ s and 2 ms) and fixed gate times (1 ms). In all cases, the decays were strictly monoexponential.

Materials. Ammonium acetate (Lancaster), 3-benzoylacrylic acid (Aldrich), and reagent-grade solvents were used as received. *N*-(2-Pyridacyl)pyridinium iodide⁴⁸ and [Pd(PhCN)₂Cl₂]⁴⁹ were prepared according to literature procedures. The

syntheses of the ligands 4-(4'-carboxyphenyl)-6-phenyl-2,2'-bipyridine (HL2)¹⁷ and 4-(4'-hydroxyphenyl)-6-phenyl-2,2'-bipyridine (HL3)¹⁸ were reported previously. The preparation of ligand 4-carboxy-6-phenyl-2,2'-bipyridine (HL1) was recently reported by our group,⁴⁶ although the synthetic details were not given at that time.

4-Carboxy-6-phenyl-2,2'-bipyridine (HL1). A stirred mixture of 3-benzoylacrylic acid (580 mg, 3.29 mmol), *N*-(2-pyridacyl)pyridinium iodide (1.03 g, 3.29 mmol), and a 10-fold excess of ammonium acetate (2.54 g) in methanol (10 mL) was refluxed for 8 h. After the resulting red-black solution was cooled to ambient temperature it was diluted with water (100 mL) and acidified with concentrated HCl to pH \approx 2. The crude solid formed was filtered off and recrystallized from methanol and water to yield the product as small gray needles in a 76% yield. Mp: 255 °C. IR (KBr, cm⁻¹): ν (COO) 1709. ¹H NMR (CD₃OD, 300 MHz): δ 8.99 (d, *J* = 1.2 Hz, 1H, central pyridine), 8.88 (br d, *J* = 5 Hz, 1H, external pyridine), 8.81 (d, *J* = 8.0 Hz, 1H, external pyridine), 8.58 (d, *J* = 1.2 Hz, 1H, central pyridine), 8.42 (m, 2H, phenyl), 8.19 (ddd, *J* = 7.9, 7.5, 1.8 Hz, 1H, external pyridine), 7.76–7.65 (m, 4H, external pyridine + phenyl). Anal. Calcd for C₁₇H₁₂N₂O₂: C, 73.90; H, 4.38; N, 10.24. Found: C, 73.47; H, 4.08; N, 10.51.

[Pd(L1)Cl] (1). A solution of [Pd(PhCN)₂Cl₂] (82 mg, 0.215 mmol) in benzene (4 mL) was added to a suspension of HL1 (60 mg, 0.215 mmol) in methanol (5 mL). The mixture was then refluxed for 7 h, affording a yellow microcrystalline precipitate. The solid was collected by filtration, washed with methanol and diethyl ether, and vacuum-dried. Yield: 79 mg (87%); mp > 350 °C. IR (KBr, cm⁻¹): ν (COO) 1707. ¹H NMR (DMSO-*d*₆, 300 MHz): δ 8.74 (d, *J* = 8.0 Hz, 1H, external pyridine), 8.71 (br d, *J* = 5 Hz, 1H, external pyridine), 8.59 (s, 1H, central pyridine), 8.35 (s, 1H, central pyridine), 8.34 (br t, 1H, external pyridine), 7.89 (m, 1H, external pyridine), 7.81 (br m, 1H, metalated phenyl), 7.60 (br m, 1H, metalated phenyl), 7.24–7.17 (m, 2H, metalated phenyl). Anal. Calcd for C₁₇H₁₁ClN₂O₂Pd·H₂O: C, 46.92; H, 3.01; N, 6.72. Found: C, 47.33; H, 2.64; N, 6.39.

[Pd(L2)Cl] (2). The procedure was similar to that adopted for **1** (reflux time, 4 h). The bright yellow microcrystalline product was obtained in 88% yield. Mp > 350 °C. IR (KBr, cm⁻¹): ν (COO) 1684, 1697. ¹H NMR (DMSO-*d*₆, 300 MHz): δ 8.82 (d, *J* = 8.0 Hz, 1H, external pyridine), 8.74 (br d, *J* = 5 Hz, 1H, external pyridine), 8.69 (s, 1H, central pyridine), 8.48 (s, 1H, central pyridine), 8.38 (br t, 1H, external pyridine), 8.32 (d, *J* = 8.5 Hz, 2H, phenyl), 8.23 (d, *J* = 8.5 Hz, 2H, phenyl), 7.95 (dd, *J* = 7.2, 1.7 Hz, 1H, metalated phenyl), 7.90 (m, 1H, external pyridine), 7.61 (dd, *J* = 7.2, 1.6 Hz, 1H metalated phenyl), 7.26–7.17 (m, 2H, metalated phenyl). Anal. Calcd for C₂₃H₁₅ClN₂O₂Pd: C, 56.01; H, 3.07; N, 5.68. Found: C, 55.62; H, 3.05; N, 5.58.

[Pd(L3)Cl] (3). A golden yellow solution was obtained upon addition of a solution of [Pd(PhCN)₂Cl₂] (71 mg, 0.185 mmol) in benzene (4 mL) to a stirred suspension of HL3 (60 mg, 0.185 mmol) in methanol (4 mL). Stirring of the solution at room temperature resulted in the formation of a yellow precipitate within 1 h. The microcrystalline solid was filtered off, washed with diethyl ether, and vacuum-dried. Yield: 82 mg (95%). Mp > 350 °C. ¹H NMR (DMSO-*d*₆, 300 MHz): δ 10.0 (s, 1H, OH), 8.62 (d, 1H, *J* = 8.0 Hz, external pyridine), 8.53 (br d, *J* = 4.9 Hz, 1H, external pyridine), 8.37 (s, 1H, central pyridine), 8.17 (ddd, *J* = 7.8, 7.1, 1.5 Hz, 1H, external pyridine), 8.13 (br s, 1H central pyridine), 7.91 (d, *J* = 8.7 Hz, 2H, phenyl), 7.72 (dd, *J* = 7.2, 1.7 Hz, 1H, metalated phenyl), 7.68 (m, 1H, external pyridine), 7.41 (dd, *J* = 7.2, 1.6 Hz, 1H, metalated phenyl), 7.02–6.93 (m, 2H, metalated phenyl), 6.86 (d, *J* = 8.7 Hz, 2H, phenyl). Anal. Calcd for C₂₂H₁₅ClN₂OPd: C, 56.80; H, 3.25; N, 6.02. Found: C, 56.40; H, 3.16; N, 6.41.

(48) Treffert-Ziemelis, S. M.; Golus, J.; Strommen, D.; Kincaid, J. R. *Inorg. Chem.* **1993**, *32*, 3890.

X-ray Crystallographic Study of 1. Single-crystal diffraction data for complex **1** were recorded on a Siemens R3m/V diffractometer using graphite-monochromated Mo K α radiation ($\lambda = 0.71073$ Å). Lorentz and polarization corrections were applied to the data. An empirical absorption correction based on Ψ scans was also applied. Crystallographic data and data collection parameters are summarized in Table 2.

The structure solution (direct methods) and full-matrix least-squares refinements based on F^2 were performed with SHELXS/L programs of the SHELXTL-NT software package (Version 5.10).⁵⁰ The weighting scheme used in the last refinement cycle was $w^{-1} = [\sigma^2(F_o)^2 + (aP)^2 + bP]$ where $P = [2F_c^2 + \text{Max}(F_o^2, 0)]/3$, with $a = 0.071$ and $b = 0.82$. All non-hydrogen atoms were refined anisotropically. The observed hydrogen atoms of the cocrystallized water molecule were

(49) Karash, M. S.; Seyler, R. C.; Mayo, F. R. *J. Am. Chem. Soc.* **1938**, *60*, 882.

(50) SHELXTL-NT crystal structure analysis package; Bruker AXS Inc.: Madison, WI, 1999; Version 5.10.

included in the refinement at fixed O–H and H \cdots H distances (0.96 and 1.48 Å). The carboxylic hydrogen atom was revealed in difference Fourier maps, and it was treated as a riding atom with an O–H distance of 0.82 Å. The remaining hydrogen atoms were included as idealized atoms riding on the respective carbon atoms with C–H bond lengths appropriate to the carbon atom hybridization.

Acknowledgment. Financial support from the Italian Ministero dell'Istruzione, dell'Università e della Ricerca (MIUR), is gratefully acknowledged.

Supporting Information Available: Details of crystal structure solution and refinement, complete lists of atomic coordinates, bond lengths and angles, anisotropic thermal parameters, torsion angles, and hydrogen bond parameters. This material is available free of charge via the Internet at <http://pubs.acs.org>.

OM020204J